International Journal of Applied Glass Science, 7 [4] 513–523 (2016)
DOI:10.1111/ijag.12189

INTERNATIONAL JOURNAL OF
Applied Glass
SCIENCE

GeS_2–Ga_2S_3–LiCl Glass System: Electrical Conductivity and Structural Considerations

Solenn Cozic, Antoine Bréhault, and David Le Coq*

Institut des Sciences Chimiques de Rennes, Eq. Verres et Céramiques, UMR 6226 CNRS, Univ. Rennes 1, Rennes Cedex 35042, France

Takeshi Usuki

Department of Material and Biological Chemistry, Faculty of Science, Yamagata University, Yamagata 990-8560, Japan

Chalcogenide samples were synthesized by melting-quenching method in the GeS_2–Ga_2S_3–LiCl system to determine its vitreous domain. Different series were investigated by varying either the GeS_2/Ga_2S_3 ratio or the molar content of LiCl. The study allows to establish that a maximum of 20 mol% of LiCl can be added in the glass composition. The glass transition and onset crystallization temperatures (T_g and T_x) and density have been determined and the thermal stability is discussed following the ΔT (T_x–T_g) parameter. The electrical conductivity of glasses increases with the LiCl content and reaches a maximum of 1.2 μS/cm at room temperature. Finally, correlations between the conductivity and the structure analyzed by Raman spectroscopy were highlighted.

Keywords: *AC conductivity; electrical properties, sulfide; glass forming systems, structure, ionic conductivity*

Introduction

Highly conducting glasses were first reported by Kunze in 1973 in the AgI–Ag_2SeO_4 system.[1] After that, it was suggested that high ionic mobility could be reached in glassy-like structures. This specificity can be related to the isotropic properties and no grain boundaries in glasses, explaining the higher conductivity values generally observed than in their crystal counterparts.[2] Electrical conductivity in alkali chalcogenide glasses has also been intensively investigated during last decades in different glassy systems.[3–10] Due to their specific electrical conductivity properties, these ones can be suitable to be used as solid-state electrolytes, which are attracting for their safety and reliability.[11,12] More specifically, sulfur- and lithium-based systems are great of interest because of their low electronic contribution to the electrical conductivity as, for example, in glasses such as Li_2S–SiS_2, GeS_2, P_2S_5, B_2S_3, or AsS_3.[4–7]

However, these systems are quite unstable forward decomposition in air atmosphere. To thwart this

*david.lecoq@univ-rennes1.fr

drawback, the GeS_2–Ga_2S_3 matrix has been chosen as a glass host because GeS_2 is one of the more thermally stable chalcogenide glass former and because Ga_2S_3, integrated as a glass intermediate, uses to extend the glass-forming range. Moreover, it was reported that alkali halides (MX) could be incorporated to this glass matrix,[13–16] without inducing drastic instability, especially at low or intermediate MX content in comparison with other systems. Among halides, alkali chloride glasses are easier to prepare and have a better atmospheric stability.[17] Otherwise, addition of halogenide combined to charge carrier (e.g., Li^+, Na^+ or Ag^+) is reported to induce a drastic increase in ionic conductivity,[16] especially with Li halide, as shown in several studies.[16–19] In this context, the study of LiCl addition into the GeS_2–Ga_2S_3 glass matrix is very promising.

In this paper, the glass-forming range of the GeS_2–Ga_2S_3–LiCl system is determined and macroscopic properties such as density and characteristic temperatures of glasses prepared are examined. The composition dependence of conductivity of chalcohalide glasses synthesized is studied by impedance spectroscopy and potentiostatic chronoamperometry. Raman spectroscopy is used to discuss the influence of both LiCl addition and GeS_2/Ga_2S_3 ratio on local structure. Finally, all these characterizations are combined to attempt to correlate the structure and the glass properties.

Experimental Methods

Glass Preparation

$[(GeS_2)_{1-y}(Ga_2S_3)_y]_{100-x}[LiCl]_x$ glasses with $0.1 \leq y \leq 0.35$ and $0 \leq x \leq 20$ were prepared by the melting-quenching method from high purity components (Ge 5N, Ga 5N, S 5N, and LiCl 2N). They were weighted in high purity argon-filled glove box in appropriate proportions and sealed under vacuum into a silica ampoule of 7 mm inner diameter and 1 mm thickness. The silica ampoule was then introduced inside a rocking furnace and the mixture was heated slowly up to a maximum temperature of 980°C. Glasses of a 4 g and 3 mm thickness were obtained by horizontally quenching the ampoule in iced-salted water. The amorphous nature of the samples was verified by X-ray diffraction (XRD) and scanning electron microscopy (SEM) analyses.

Thermal and Density Analyses

A differential scanning calorimeter (DSC Q20 Thermal Analysis) was used to characterize the thermal properties of glasses. Samples between 3 mg and 7 mg were sealed in aluminum pans. Then, the measurement was performed from room temperature up to 550°C with a heating rate of 10°C/min under nitrogen atmosphere. Characteristic temperatures including glass transition temperature (T_g) and crystallization onset temperature (T_x) were determined from DSC curves with an accuracy of ±2°C.

The density of each glass composition was estimated at room temperature by Archimedean method for several samples having a mass between 0.5 and 1 g using ethanol as immerging fluid. The molar volume was then calculated taking into account the density and the molar weight of the elements.

Impedance Spectroscopy and Potentiostatic Chronoamperometry

Before performing electrical measurements, samples were polished in regular parallelepipeds of ≈1 mm thickness with SiC polishing paper and a thin layer of gold was deposited to form blocking electrodes and to ensure good electrical contact with electrodes of the measurement cell. A pressure of approximately 80 kPa was also applied.

All measurements were performed by means of Autolab workstation (PGSTAT302N with FRA32M and ECD module) from 283 K up to 333 K with a frequency range from 1 MHz down to 1 Hz and a signal amplitude of 100 mV. Several cycles were recorded in order to evaluate the hysteresis effects that were found to be negligible. Moreover, d.c. potentiostatic measurements were also carried out with the same equipment and samples. A constant voltage of 100 mV was applied and the d.c. potentiostatic conductivity σ_{dcp} was calculated from the steady state I_∞ (at time $\rightarrow \infty$) at room temperature.

Raman Spectroscopy

Raman spectra were obtained using a Thermo Scientific DXR Raman microscope. Parallelepiped samples were excited by an incident laser of $\lambda = 523$ nm with an input power of 10 mW, where the laser was focused on the sample surface through a ×100 objec-

tive lens. A 10-second measurement was repeated ten times for one sample.

Results

Glass-Forming Region

The delimitation of the glass-forming region of the pseudo-ternary system determined from analyses by XRD and SEM of synthesized samples is depicted in Fig. 1. It is observed that a maximum of 20 mol% of LiCl can be added to obtain glasses. The limit molar contents of GeS_2 and Ga_2S_3 are 55–100% and 0–35%, respectively. We can also note that a higher ratio Ga_2S_3/GeS_2 allows a higher amount of LiCl to be present in the glass composition. To evaluate the effects of the LiCl addition or the Ga_2S_3/GeS_2 ratio on the properties of these glasses, different series have been investigated and identified as follows: A $[(GeS_2)_{0.7}(Ga_2S_3)_{0.3}]_{100-x}[LiCl]_x$, B $[(GeS_2)_{0.8}(Ga_2S_3)_{0.2}]_{100-x}[LiCl]_x$, C $[(GeS_2)_{0.9}(Ga_2S_3)_{0.1}]_{100-x}[LiCl]_x$, and D $[(GeS_2)_{1-y}(Ga_2S_3)_y]_{90}[LiCl]_{10}$ where $0.1 \leq y \leq 0.35$.

Macroscopic Properties

The characteristic temperatures including the glass transition temperature T_g and the onset crystallization temperature T_x of the synthesized glasses are given in Table I. In this pseudo-ternary system, all T_g are higher than 330°C. Their evolution as a function of the LiCl molar content x is plotted in Fig. 2a for the series A, B, and C. As shown, T_g linearly decreases with LiCl addition from 438°C down to 338°C, 436°C down to 375°C, and 434°C down to 415°C in the series A, B, and C, respectively. No any critical change of behavior between the different host glasses was observed. The only exception occurs in series C in which T_g is found to be approximately identical for glasses containing 5 mol% and 10 mol% of LiCl.

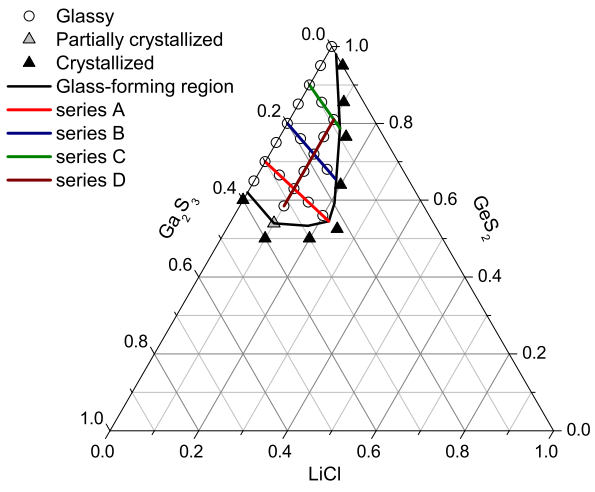

Fig. 1. Glass-forming region of the GeS_2–Ga_2S_3–LiCl pseudo-ternary system.

If the trend in T_g evolution is almost similar for all series, the Fig. 2b highlights the differences in the evolution of glass-forming ability, which is reflected by ΔT criterion (with $\Delta T = T_x - T_g$, the glass being considered as thermally stable if $\Delta T > 100$°C). Thus, the LiCl addition to the base glass is characterized by an increase in the glass-forming ability for series A and B for $0 \leq x \leq 15$ and a maximum is observed for $[(GeS_2)_{0.8}(Ga_2S_3)_{0.2}]_{85}[LiCl]_{15}$ glass ($\Delta T = 129$°C, that is to say 43°C more than for the host glass without LiCl incorporation). The series A accepts a higher molar content of LiCl ($x = 20$), but a failure in the trend previously observed appears. On the contrary, series C does not show a linear evolution of ΔT with LiCl molar content that is a consequence of the T_g evolution underlined above.

Concerning the series D, T_g does not show a monotonic evolution since a decrease is firstly observed, followed by an increase and finally another decrease (Table I). This peculiar behavior is in good agreement with other works led on the GeX_2–Ga_2X_3 (X = S, Se) pseudo-binary system, in which it is noted an analogous feature.[20,21] Indeed, the minimum of T_g is obtained for the specific composition $(GeS_2)_{83}$–$(Ga_2S_3)_{17}$ which is concordant with our results.

From the molar volume (V_M) point of view, Fig. 2c shows that whatever the series a systematic linear decrease is observed. Besides, V_M remains lower for series having more Ga_2S_3 ($V_{M\ series\ A} < V_{M\ series\ B} < V_{M\ series\ C}$).

Electrical Measurements

All series have been investigated by impedance spectroscopy. As an example, the Fig. 3 displays the Nyquist diagrams of the series A, corresponding to the frequency-dependent complex impedance data ($Z = Z' - i\,Z''$). This diagram can be divided into two parts: the semicircle, in the high- and mid-frequency region, representing the sample's impedance,

Table I. Values of Experimental Results for the Series A $[(GeS_2)_{0.7}(Ga_2S_3)_{0.3}]_{100-x}[LiCl]_x$, B $[(GeS_2)_{0.8}(Ga_2S_3)_{0.2}]_{100-x}[LiCl]_x$, C $[(GeS_2)_{0.9}(Ga_2S_3)_{0.1}]_{100-x}[LiCl]_x$, and D $[(GeS_2)_{1-y}(Ga_2S_3)_y]_{90}[LiCl]_{10}$ Including Glass Transition Temperature T_g, Onset Crystallization Temperature T_x, Density d, Electrical Conductivity at Room Temperature $log(\sigma_{298\ K})$, and Activation Energy E_σ. Thermal Stability Criterion is also Given as $\Delta T = T_x - T_g$.

	Thermal analysis			Density	Molar volume	Electric conductivity	
Sample composition	T_g (±2°C)	T_x(±2°C)	ΔT (±4°C)	d(±0.01 g/cm^3)	V_M (±0.02 cm^3/mol)	$log\ \sigma_{ac(298\ K)}$ (±0.10 S/cm)	E_σ (±0.01 eV)
Series A							
$[(GeS_2)_{0.7}(Ga_2S_3)_{0.3}]_{100-x}[LiCl]_x$							
$x = 0$	438	492	54	2.87	16.04	/	/
$x = 5$	416	475	59	2.85	15.72	−7.66	0.53
$x = 10$	391	466	75	2.83	15.39	−6.77	0.48
$x = 15$	365	449	84	2.80	15.12	−6.30	0.50
$x = 20$	338	398	60	2.76	14.88	−5.91	0.54
Series B							
$[(GeS_2)_{0.8}(Ga_2S_3)_{0.2}]_{100-x}[LiCl]_x$							
$x = 0$	436	522	86	2.80	16.39	/	/
$x = 5$	408	516	108	2.78	16.06	−7.42	0.51
$x = 10$	386	508	122	2.76	15.73	−6.56	0.52
$x = 15$	375	504	129	2.75	15.34	−6.09	0.51
Series C							
$[(GeS_2)_{0.9}(Ga_2S_3)_{0.1}]_{100-x}[LiCl]_x$							
$x = 0$	434	547	113	2.72	16.81	/	/
$x = 5$	412	505	93	2.68	16.61	−7.21	0.49
$x = 10$	415	509	94	2.65	16.33	−6.57	0.47
Series D							
$[(GeS_2)_{1-y}(Ga_2S_3)_y]_{90}[LiCl]_{10}$							
$y = 0.10$	415	509	94	2.65	16.33	−6.57	0.47
$y = 0.15$	382	492	110	2.77	15.65	−6.51	0.48
$y = 0.20$	386	508	122	2.76	15.73	−6.56	0.52
$y = 0.25$	393	496	103	2.84	15.31	−6.63	0.47
$y = 0.30$	391	466	75	2.83	15.39	−6.77	0.48
$y = 0.35$	391	454	63	2.90	15.04	−7.00	0.48

and the tail, in the low-frequency region, representing the electrode polarization. This polarization is induced by accumulation of charge carriers (here, Li^+) at the interface between the sample and the electrodes and is well known to be characteristic of ionic conductors.

The sample total resistance R is obtained by extrapolating the imaginary part Z'' of complex impedance to the Z' axis, at low-frequency area. Thus, in Fig. 3, a decrease in R is observed following the increase in the LiCl molar content. The a.c. total conductivity values σ_{ac} were calculated as follows:

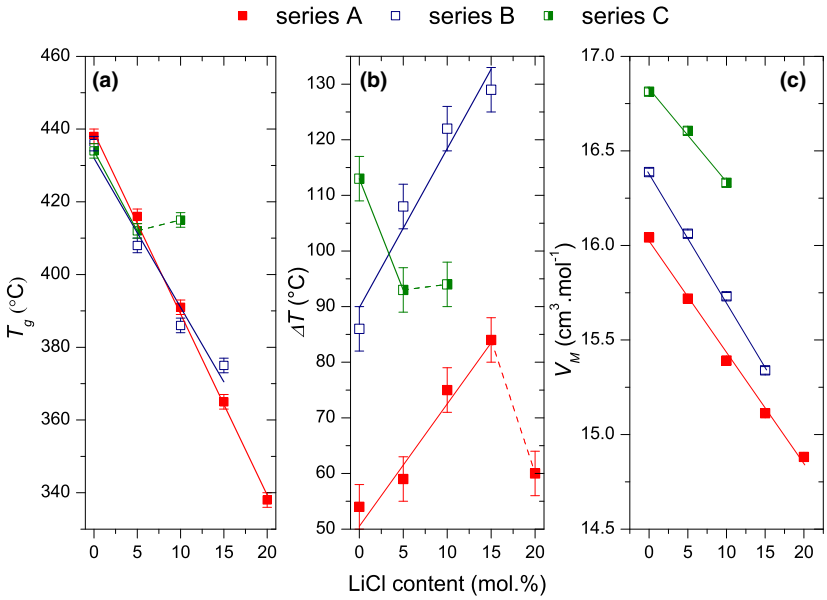

Fig. 2. Evolution of the glass transition temperature T_g(a), DT (b), and the molar volume V_M (c) as a function of the LiCl molar content for the series A, B and C.

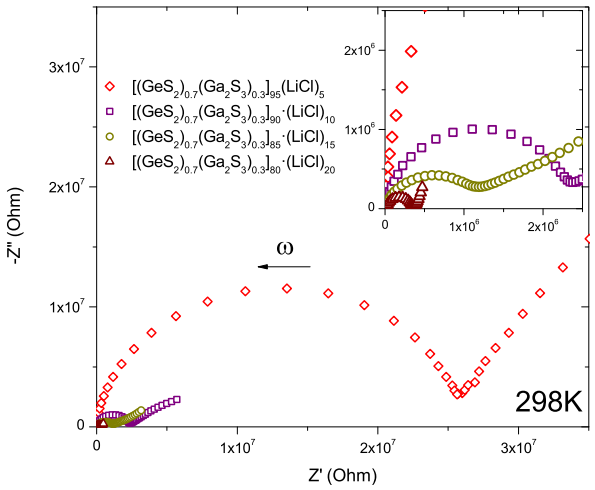

Fig. 3. Nyquist's diagrams for the samples of series A, $[(GeS_2)_{0.7}(Ga_2S_3)_{0.3}]_{100-x}[LiCl]_x$, x = 5, 10, 15 and 20 at T = 298K.

$$\sigma_{ac} = l/(R \times A) \qquad (1)$$

where l is the sample thickness and A the area of the electrodes.

The Fig. 4a displays σ_{ac} of the samples of series A, B, and C. All data series obey the Arrhenius law:

$$\sigma_{ac} = \frac{\sigma_0}{T}\exp\left(-\frac{E_a}{kT}\right) \qquad (2)$$

where σ_0 is the pre-exponential factor, $E\sigma$ the activation energy, k the Boltzmann constant, and T the temperature. By fitting these experimental data, both the room temperature conductivity σ_{298} and $E\sigma$ have been determined (Table I). Whatever the series, $E\sigma$ is very close to 0.5 eV and does not show evidence of the LiCl molar content influence on its trend. On the contrary, σ_{298} increases with the LiCl molar content for all series and its monotonic evolution is shown in Fig. 4b, following the atomic content of Li.

No evidence of the influence of GeS_2/Ga_2S_3 ratio on the value of σ_{298} is observed even if at low Li content, higher this ratio is, higher σ_{298} is. The highest value of σ_{298} equal to 1.23 µS/cm is obtained in series A for an atomic Li content of 6.1%, corresponding to the glass of series A having the highest molar content of LiCl (x = 20 mol%).

Raman Spectroscopy

The different contributions in the Raman spectra between 200 cm^{-1} and 500 cm^{-1} can be attributed to four main structural entities present in the glass net-

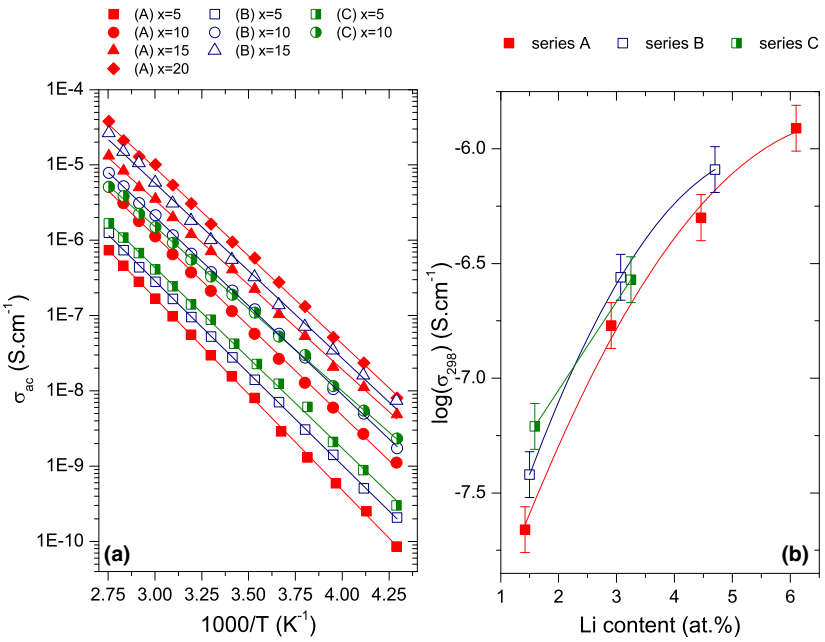

Fig. 4. (a) Reciprocal temperature dependence of the a.c. conductivity σ_{ac} for series A, B, and C. (b) Influence of the lithium atomic content on the total electrical conductivity at room temperature ($T = 298$ K) σ_{298} for the glasses of series A, B and C.

work of the studied system. These structural entities, illustrated in Fig. 5, are identified as ethane-like (ETH)[22] and triclusters (TRI) units, corner-sharing (CS) and edge-sharing (ES) tetrahedra[23,24].

Thus, the first sharp shoulder around 270 cm^{-1} can be attributed to antisymmetric stretching vibration of homopolar bonds in ETH [S_3 Ga(Ge)–Ga(Ge)S_3], which are mainly related to Ga contribution.[25–28] Next, a lower contribution is needed around 310 cm^{-1} to be able to correctly fit the Raman spectra. Masselin *et al.* have recently demonstrated that this contribution could be assigned to a TRI, which can be expressed as $[GaS_{1/3}S_{3/p}]_3$, with $P = 2$ or 3.[26,27] The most intense band around 337 cm^{-1} can be ascribed to A_1 symmetric stretching vibration of CS [$GeS_{4/2}$] and [$GaS_{4/2}$] units.[28] The two bands located at 368 cm^{-1} and 431 cm^{-1} are related to ES connections between [GeS_4] and [GaS_4] tetrahedrons and the first band is the A_{1c} companion of A_1 vibration in CS tetrahedrons. Around 394 cm^{-1}, *ab initio* calculations have demonstrated that this feature is related to both CS and ES tetrahedrons contributions.[29,30] We can also notice the low contribution of S–S homopolar bonds near 480 cm^{-1}, which is present in S_8 rings or S_n chains as reported in the literature for S-rich samples.[24,30–33]

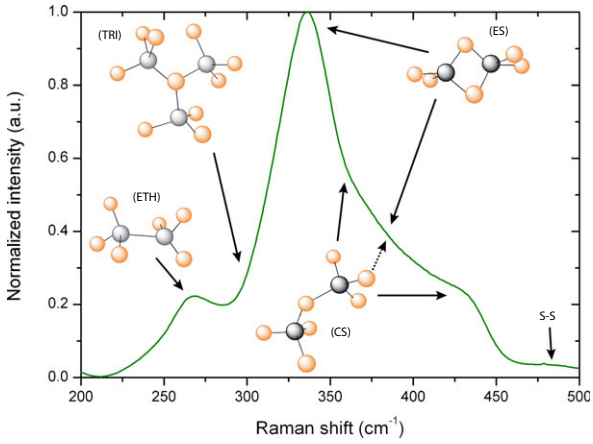

Fig. 5. Typical Raman spectrum of a glass belonging to the GeS_2–Ga_2S_3–LiCl system and contributions of four main structural entities: ethane-like (ETH) and triclusters (TRI) units, corner-sharing (CS) and edge-sharing (ES) tetrahedrons. S atoms are represented by orange circles. The gray circlesare mainly devoted to Ga (even if Ge-based units are possible) and the black circlesare mainly devoted to Ge (even if Ga-based units are possible).

Figures 6a and b shows that LiCl addition into compositions of the series A and B does not induce important change on the repartition of structural enti-

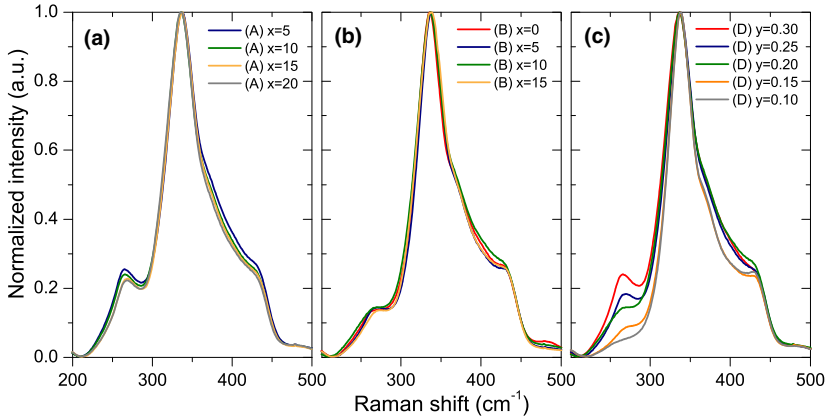

Fig. 6. Evolution of the Raman spectra of glasses following the LiCl mol% content x for (a) series A $[(GeS_2)_{0.7}(Ga_2S_3)_{0.3}]_{100-x}[LiCl]_x$ and (b) series B $[(GeS_2)_{0.8}(Ga_2S_3)_{0.2}]_{100-x}[LiCl]_x$, and with Ga_2S_3 content y for (c) series D $[(GeS_2)_{1-y}(Ga_2S_3)_y]_{90}[LiCl]_{10}$.

ties contribution, excepted for series A where ETH exhibits a slight decrease and shift forward higher wavenumber with higher LiCl content.

On the contrary, the spectra of the series D $[(GeS_2)_{1-y}(Ga_2S_3)_y]_{90}[LiCl]_{10}$, $0 \leq y \leq 0.30$, displayed in Fig. 6c, show that a higher amount of Ga_2S_3 leads to the increase in ETH contribution into the local structure of the glass.

Discussion

The GeS_2–Ga_2S_3–LiCl system exhibits a wider glass-forming region than the reported one by Tver'yanovich *et al.* in which the maximum of LiCl content does not exceed 15 mol%.[18] This difference can probably be explained by the difference between the quenching method since in our experimental conditions, the samples were cooled very quickly by immerging them in iced-salted water, while Tver'yanovich *et al.* have operated in air or water.

Not surprisingly, for each series, addition of LiCl leads to a decrease in T_g, accompanied by a ΔT increase. The same phenomenon was observed in GeS_2–Ga_2S_3 system with insertion of NaCl or CsCl.[17,34] This behavior happens consequently to the Cl introduction, breaking Ge–S and Ga–S bonds, and leading to a decrease in the glass network connectivity. Otherwise, in literature the formation of $GaS_{3/2}Cl^-$ formed to retain the fourfold coordination of Ga decreases the glass connectivity and is assumed to favor the glass formation.[18,34] But as demonstrated later, the ETH based on Ga–Ga homopolar bond ($Ga_2S_{6/2}$) has to be preferentially considered comparatively to the tetrahedron unit $GaS_{4/2}$. In this case, a similar reasoning by replacing $GaS_{3/2}Cl^-$ by $Ga_2S_{5/2}Cl^-$ leads to an identical explanation. Nevertheless, the decrease in T_g is more pronounced than the increase in ΔT, meaning that the addition of LiCl also facilitates the crystallization.

The lowest ΔT between series C, B, and A, in the GeS_2–Ga_2S_3 eutectic system (for $x = 0$ mol%), corresponding to a decrease in the glass-forming ability, depicted in Fig. 2b, can be explained by the addition of Ga_2S_3, which is not a glass-former component.

Moreover, some failures in the T_g and ΔT trends appear in series A and C. It is assumed that this feature is due to the composition of the glasses that is located very close from the limit of the glass-forming region, and consequently, they show a lower stability. To confirm this assumption, samples of series A have been kept in open air to follow their stability. So the low stability of glass with the highest content in LiCl in series C ($x = 20$ mol%) has been highlighted. The gradual decomposition of this sample has been observed by firstly a progressive gain of weight due to hydration and finally to its transformation into white powder. On the contrary, sample compositions with $x = 0$ and 10 mol% did not show any sign of decomposition after 4 months in the open air.

The general decrease in sample density with LiCl addition can be explained by its lowest density ($d = 2.07$ g/cm^3) compared to the host glasses (2.87,

2.80, and 2.72 g/cm^3 for series A, B, and C with $x = 0$, respectively). Also, we can observe in Fig. 2c that the slope of the molar volume decrease is quite different following the GeS_2/Ga_2S_3 ratio, reflecting its influence on the structure of the host glass. Consequently, the difference observed for the decrease in both density and molar volume between series A, B, and C can be ascribed to a synergetic effect of LiCl addition and Ga_2S_3/GeS_2 ratio.

The measurements performed by impedance spectroscopy allow to determine the total electrical conductivity (σ_{ac}), corresponding to the summation of the electronic and ionic conductivity. The regular shape of Nyquist's plots in Fig. 3 confirms a single dominant conduction mechanism of glasses. For many applications, it is very important to be able to distinguish the electronic and ionic parts. Even if sulfide glasses are well known to be ionic conductors, an estimation of the electronic contribution to the total electrical conductivity was carried out by potentiostatic chronoamperometry for $[(GeS_2)_{0.7}(Ga_2S_3)_{0.3}]_{90}[LiCl]_{10}$ and $[(GeS_2)_{0.8}(Ga_2S_3)_{0.2}]_{90}[LiCl]_{10}$ compositions at room temperature. Measurements were also carried out for similar compositions using selenium instead of sulfur as chalcogen. Figure 7 shows typical Nyquist's diagrams and d.c. potentiostatic chronoamperometry obtained for $[(GeY_2)_{0.8}(Ga_2Y_3)_{0.2}]_{90}[LiCl]_{10}$ with Y = Se and S. As expected, the selenide-based glass does not exhibit tail at low-frequency region (Fig. 7a), meaning that the main contribution to the total electrical conductivity should be electronic. Moreover, the Fig. 7b shows that the residual current after an infinite time is drastically increased when the sample is a selenide-based glass compared to sulfide-based one. The d.c. potentiostatic conductivity σ_{dcp}, which can be assimilated to the electronic conductivity, was then calculated for the four samples using relation (3),

$$\sigma_{dcp} = \frac{I_\infty \times l}{U \times A} \tag{3}$$

where I_∞ is the current when time $t \to \infty$, U is the applied voltage, l is the sample thickness, and A is the area of electrodes.

All calculated values are reported in Table II. As expected, electronic contribution σ_{dcp} to total conductivity was found to be negligible for sulfide samples (<0.1%). Thus, the total conductivity σ_{ac} determined previously will be assimilated to an ionic conductivity in our sulfide system. In the case of selenide samples, a major electronic contribution to total electric conductivity is underscored. For a same composition, the electronic contribution to total conductivity is much more important than in sulfide glasses.

Finally, the addition of LiCl in the glass composition is directly correlated with the increase in Li^+ charge carriers and consequently to the ionic conductivity and total electrical conductivity increase. The dependence on the room temperature conductivity following the GeS_2/Ga_2S_3 ratio has already been reported in the literature for similar systems. Never-

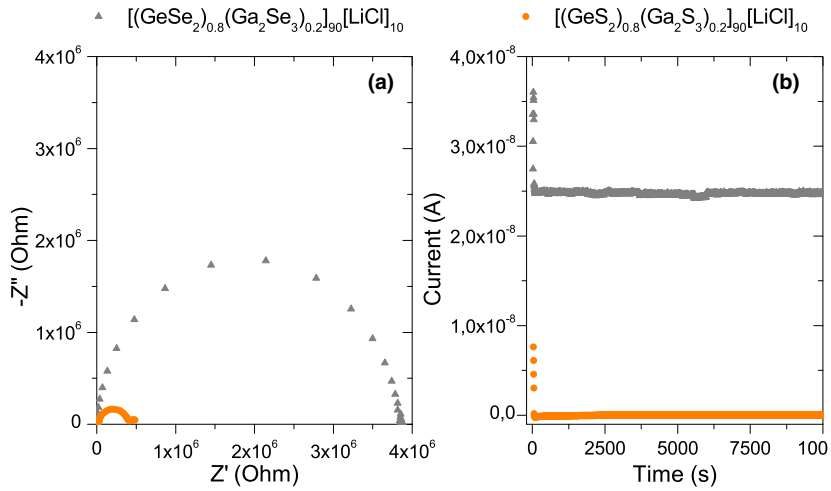

Fig. 7. Influence of the chalcogen element (S or Se) on the Nyquist's plot (a) and the potentiostaticchronoamperometry (b) for $[(GeY_2)_{0.8}(Ga_2Y_3)_{0.2}]_{90}[LiCl]_{10}$ (Y = Se, S).

Table II. d.c. Potentiostatic Conductivity σ_{dcp} Contribution to the Total Electric Conductivity σ_{ac} at Room Temperature.

Glass composition	σ_{ac} (298 K) (S/cm)	σ_{dcp} (298 K) (S/cm)	% σ_{dcp}
$[(GeS_2)_{0.7}(Ga_2S_3)_{0.3}]_{90}[LiCl]_{10}$	1.7×10^{-7}	1.48×10^{-10}	0.09%
$[(GeSe_2)_{0.7}(Ga_2Se_3)_{0.3}]_{90}[LiCl]_{10}$	1.5×10^{-9}	7.98×10^{-10}	53%
$[(GeS_2)_{0.8}(Ga_2S_3)_{0.2}]_{90}[LiCl]_{10}$	2.8×10^{-7}	1.18×10^{-10}	0.04%
$[(GeSe_2)_{0.8}(Ga_2Se_3)_{0.2}]_{90}[LiCl]_{10}$	8.0×10^{-8}	6.90×10^{-8}	86%

theless, they usually observe a reverse behavior, consisting in an increase in conductivity when the Ga_2S_3 content is higher. Generally, they attribute this feature to the elimination of nonbridging sulfur (NBS) and formation of weak bonds between $[GaS_{4/2}]^-$ units and Li^+.[35–38] In our experiments, the effect of the GeS_2/Ga_2S_3 ratio on the conductivity is found to be relatively negligible. This could be the result of the preferential formation of ETH, instead of $GaS_{4/2}$ units of the above structural considerations. Indeed, to quantify this trend, Raman spectra were fitted as shown in Fig. 8 using the 6 main contributions underlined previously. In the fitting procedure, every contribution of the identified vibrational modes is represented by a Gaussian function. The fitting result is expressed by the red line and the residue is shown at the bottom. The results of the relative contribution distribution as a function of the GeS_2/Ga_2S_3 substitution rate (y) are illustrated in Fig. 9. It is found that the increase in Ga_2S_3 content is mainly supported by the apparition of supplementary ETH in proportion, whereas the other units are weakly affected even if the population of TRI seems to be also slightly increased. In other words, structurally speaking, the addition of Ga_2S_3 in the composition is essentially characterized by an increase in ETH instead of $GaS_{4/2}$, meaning that the formation of new $GaS_{4/2}$ using NBS has not to be considered. Consequently, the effect of the GeS_2/Ga_2S_3 ratio on the conductivity remains negligible.

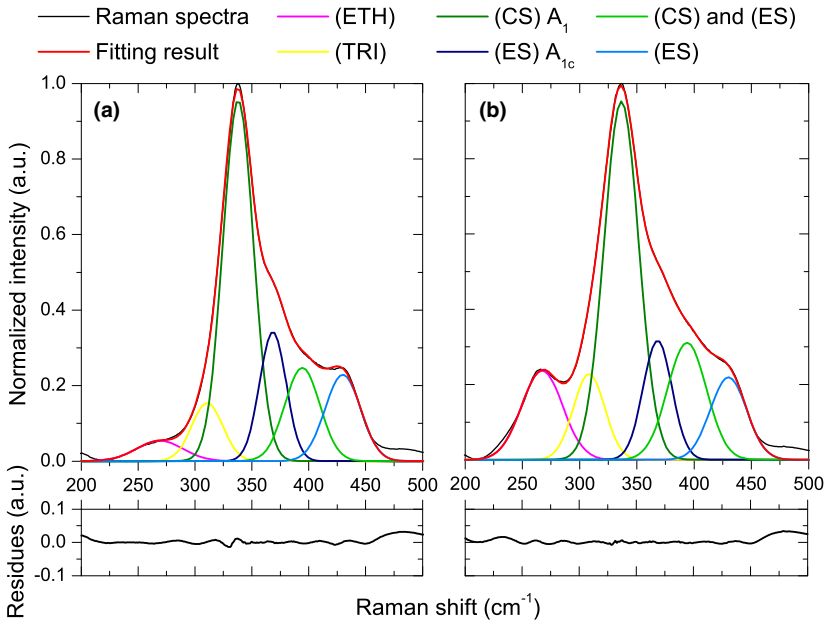

Fig. 8. Decomposition of Raman spectra for (a) $[(GeS_2)_{0.9}(Ga_2S_3)_{0.1}]_{90}[LiCl]_{10}$ and (b) $[(GeS_2)_{0.7}(Ga_2S_3)_{0.3}]_{90}[LiCl]_{10}$ glass samples.

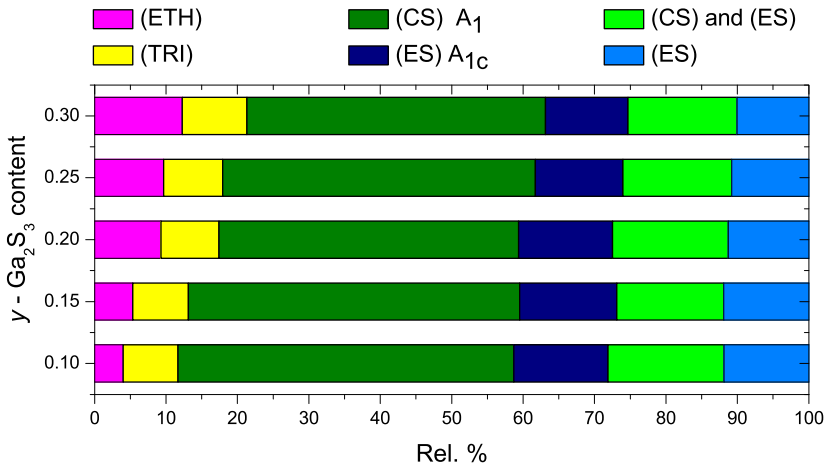

Fig. 9. Evolution of the relative contribution distribution of the structural units for glasses of the series D.

At last, the slight decrease in ETH band with LiCl content in series A (Fig. 6a) is assumed to be related to the destruction of the Ga-Ga homopolar bonds in ETH due to the Cl addition and the formation of some $GaS_{3/2}Cl^-$ units.[15,39,40]

Raman shift of ETH contribution following the GeS_2/Ga_2S_3 ratio is well described in literature. It is due to the relative position of the 2 ETH based on either Ge ($S_3Ge–Ge–S_3$) or Ga (S_3 Ga–Ga–S_3) at 257 cm^{-1} and 267 cm^{-1}.[15,41] Nevertheless, here this wavenumber shift occurs at a constant GeS_2/Ga_2S_3 ratio and has to be related to the substitution of the S by Cl and the breathing mode contribution of $GaS_{3/2}Cl^-$ structure subunits around 320 cm^{-1}[15]

At this investigation level, the ionic conduction has to be correlated with both the number of charge carriers (Li^+) and the structural consideration due to the presence of ETH in our glasses. These conclusions should be supported by other structural investigation, such as EXAFS experiments to confirm the presence of Ga–Ga homopolar bond. Other supplementary structural studies including Li NMR spectroscopy and neutron diffraction with isotopic Li substitution could also inquire on the Li diffusion mechanisms in this system.

Conclusion

The GeS_2–Ga_2S_3 glass matrix allows a maximum of 20 mol% of LiCl to be added in the composition. It was also shown that at low LiCl concentration, the glasses possess good thermal and ambient air stabilities. The maximum electrical conductivity due to the Li^+ ion mobility in the glass network has been measured at 1.26 μS/cm. The structure of the investigated glasses by Raman spectroscopy is mainly characterized by an increase in ETH if the GeS_2/Ga_2S_3 ratio is decreasing. In this context, it has been highlighted that the electrical conductivity was not affected because the addition of Ga_2S_3 is not characterized by the presence of supplementary $GaS_{4/2}$ tetrahedrons and nonbridging sulfur.

References

1. D. Kunze, "Silver Ion Conducting Electrolyte with Glass-Like Structure;" *Fast ion Transport in Solids*, ed., W. Van Gool, North Holland, Amsterdam 405–408 (1973).
2. T. Minami, "Recent Progress in Superionic Conducting Glasses," *J. Non-Cryst. Solids*, 95–96 [Part 1] 107–118 (1987).
3. J. L. Adam *et al.*, "Chalcogenide Glasses: Preparation, Properties and Applications;" *Chalcogenide Glasses*, eds., J.-L. Adam and X. Zhang. Woodhead Publishing, Cambridge, 169–208, 2014.
4. A. Pradel, and M. Ribes, "Lithium Chalcogenide Conductive Glasses," *Mater. Chem. Phys.*, 23 [1–2] 121–142 (1989).
5. R. Mercier, J.-P. Malugani, B. Fahys, and G. Robert, "Proceedings of the International Conference on Fast Ionic Transport in Solids Superionic conduction in Li_2S-P_2S_5-LiI - glasses," *Solid State Ion.*, 5 663–666 (1981).
6. M. Kbala, M. Makyta, A. Levasseur, and P. Hagenmuller, "Characterization and Electrical Behavior of New Lithium Chalcoborate Thin Films," *Solid State Ion.*., 15 [2] 163–169 (1985).
7. J. H. Kennedy, and Z. M. Zhang, "Further Characterization of SiS_2–Li_2S Glasses Doped with Lithium Halide," *J. Electrochem. Soc.*, 135 [4] 859–862 (1988).
8. S. Cui, D. Le Coq, C. Boussard-Plédel, and B. Bureau, "Electrical and Optical Investigations in Te–Ge–Ag and Te–Ge–AgI Chalcogenide Glasses," *J. Alloy. Compd.*, 639 173–179 (2015).
9. S. Stehlik *et al.*, "Conductivity in Ag–As–S(Se, Te) Chalcogenide Glasses," *Solid State Ion.*, 181 [37–38] 1625–1630 (2010).
10. H. Krebs, and P. Fischer, "Electrical Conductivity of Melts and their Ability to Form Glasses in System Ge+As+Te," *Discuss. Faraday Soc.*, 1970 [50] 35–44 (1971).

11. J. M. Tarascon, and M. Armand, "Issues and Challenges Facing Rechargeable Lithium Batteries," *Nature*, 414 [6861] 359–367 (2001).
12. K. B. Hueso, M. Armand, and T. Rojo, "High Temperature Sodium Batteries: Status, Challenges and Future Trends," *Energy Environ. Sci.*, 6 [3] 734–749 (2013).
13. C. G. Lin *et al.*, "Second-order Optical Nonlinearity and Ionic Conductivity of Nanocrystalline GeS_2–Ga_2S_3–LiI Glass-Ceramics with Improved Thermo-Mechanical Properties," *Phys. Chem. Chem. Phys.*, 12 [15] 3780–3787 (2010).
14. E. G. Nedoshovenko, E. Y. Turkina, Y. S. Tveryanovich, and Z. U. Borisova, "Glass-Formation and Components Interaction in the System GeS_2–Ga_2S_3–NaCl," *Vestnik Leningradskogo Universiteta Seriya Fizika Khimiya*, 4 [2] 52–57 (1986).
15. A. Tverjanovich, Y. S. Tveryanovich, and S. Loheider, "Raman Spectra of Gallium Sulfide based Glasses," *J. Non-Cryst. Solids*, 208 [1-2] 49–55 (1996).
16. W. L. Yao, and S. W. Martin, "Ionic Conductivity of Glasses in the $MI+M_2S+(0.1Ga_2S_3+0.9GeS_2)$ System (M=Li, Na, K and Cs)," *Solid State Ion.*, 178 [33-34] 1777–1784 (2008).
17. A. Brehault *et al.*, "Influence of NaX (X=I or Cl) Additions on GeS_2–Ga_2S_3 Based Glasses," *J. Solid State Chem.*, 220 238-244 (2014).
18. Y. S. Tver'yanovich, V. V. Aleksandrov, I. V. Murin, and E. G. Nedoshovenko, "Glass-Forming Ability and Cationic Transport in Gallium Containing Chalcohalide Glasses," *J. Non-Cryst. Solids*, 256&257 237-241 (1999).
19. J. Kolár *et al.*, "Ion Conductive Chalcohalide Glasses in LiI–Ga_2S_3–GeS_2 System," *J. Non-Cryst. Solids*, 357 [11–13] 2223–2227 (2011).
20. A. W. Mao, B. G. Aitken, R. E. Youngman, D. C. Kaseman, and S. Sen, "Structure of Glasses in the Pseudobinary System Ga2Se3-GeSe2: Violation of Chemical Order and 8-N Coordination Rule," *J. Phys. Chem. B*, 117 [51] 16594–16601 (2013).
21. L. Cai, "Molecular Structure of $(Ga_2S_3)_x(GeS_2)_{1-x}$ Glasses by Raman Scattering and T-modulated DSC," Master thesis - University of Cincinnati - USA (2003).
22. H. Guo, Y. Zhai, H. Tao, G. Dong, and X. Zhao, "Structure and Properties of GeS_2–Ga_2S_3–CdI_2 Chalcohalide Glasses," *Mater. Sci. Eng.: B*, 138 [3] 235–240 (2007).
23. K. Miyauchi, J. Qiu, M. Shojiya, Y. Kawamoto, and N. Kitamura, "Structural Study of GeS_2 Glasses Permanently Densified Under High Pressures Up to 9 GPa," *J. Non-Cryst. Solids*, 279 [2-3] 186–195 (2001).
24. G. Lucovsky, F. L. Galeener, R. C. Keezer, R. H. Geils, and H. A. Six, "Structural Interpretation of Infrared and Raman-Spectra of Glasses in Ally System $Ge_{1-x}S_x$," *Phys. Rev. B*, 10 [12] 5134–5146 (1974).
25. T. Haizheng, Z. Xiujian, J. Chengbin, Y. Hui, and M. Shun, "Raman Scattering Studies of the GeS_2–Ga_2S_3–CsCl Glassy System," *Solid State Commun.*, 133 [5] 327–332 (2005).
26. A. Cuisset, F. Hindle, J. Laureyns, and E. Bychkov, "Structural Analysis of $xCsCl(1-x)Ga_2S_3$ Glasses by Means of DFT Calculations and Raman Spectroscopy," *J. Raman Spectrosc.*, 41 [9] 1050–1058 (2010).
27. P. Masselin, D. Le Coq, A. Cuisset, and E. Bychkov, "Spatially Resolved Raman Analysis of Laser Induced Refractive Index Variation in Chalcogenide Glass," *Opt. Mater. Express*, 2 [12] 1768–1775 (2012).
28. J. Heo, J. M. Yoon, and S. Y. Ryou, "Raman Spectroscopic Analysis on the Solubility Mechanism of La^{3+} in GeS_2-Ga_2S_3 Glasses," *J. Non-Cryst. Solids*, 238 [1-2] 115–123 (1998).
29. S. Blaineau, and P. Jund, "Vibrational Signature of Broken Chemical Order in a GeS_2 Glass: A Molecular Dynamics Simulation," *Phys. Rev. B*, 69 [6] 7 (2004).
30. K. Jackson, A. Briley, S. Grossman, D. V. Porezag, and M. R. Pederson, "Raman-Active Modes of a-$GeSe_2$ and a-GeS_2: A First-Principles Study," *Phys. Rev. B*, 60 [22] R14985–R14989 (1999).
31. S. Sugai, "Stochastic Random Network Model in Ge and Si Chalcogenide Glasses," *Phys. Rev. B*, 35 [3] 1345–3161 (1987).
32. P. Boolchand, J. Grothaus, M. Tenhover, M. A. Hazle, and R. K. Grasselli, "Structure of GeS_2 Glass – Spectroscopy Evidence for Broken Chemical Order," *Phys. Rev. B*, 33 [8] 5421–5434 (1986).
33. A. Ibanez, M. Bionducci, E. Philippot, L. Descôtes, and R. Bellissent, "Structural Properties of Sulphur-Enriched GeSx Binary Glasses by Neutron Scattering," *J. Non-Cryst. Solids*, 202 [3] 248–252 (1996).
34. P. Masselin *et al.*, "CsCl Effect on the Optical Properties of the $80GeS_2$–$20Ga_2S_3$ Base Glass," *Appl. Phys. A-Mater. Sci. Process.*, 106 [3] 697–702 (2012).
35. J. Saienga, and S. W. Martin, "The Comparative Structure, Properties, and Ionic Conductivity of $LiI+Li_2S+GeS_2$ Glasses Doped with Ga_2S_3 and La_2S_3," *J. Non-Cryst. Solids*, 354 [14] 1475–1486 (2008).
36. J. Saienga, Y. Kim, B. Campbell, and S. W. Martin, "Preparation and Characterization of Glasses in the $LiI+Li_2S+GeS_2+Ga_2S_3$ System," *Solid State Ion.*, 176 [13–14] 1229–1236 (2005).
37. D. S. Patil, M. S. Konale, J. Kolar, K. Shimakawa, V. Zima, and T. Wagner, "Ionic Conductivity Study of LiI-Ga_2S_3-GeS_2 Chalcogenide Glasses Using a Random-Walk Approach," *Pure Appl.* Chem., 87 [3] 249–259 (2015).
38. M. Yamashita, and H. Yamanaka, "Formation and Ionic Conductivity of Li_2S–GeS_2–Ga_2S_3 Glasses and thin Films," *Solid State Ion.*, 158 [1–2] 151–156 (2003).
39. M. Letoullec, P. S. Christensen, J. Lucas, and R. W. Berg, "A New Family of Vitreous Materials - the Cesium Aluminium or Gallium Thiohalide Glasses," *Mater. Res. Bull.*, 22 [11] 1517–1523 (1987).
40. R. W. Berg, and N. J. Bjerrum, "Raman Study of Gallium Chlorosulphides in Chloride Melts," *Polyhedron*, 2 [3] 179–181 (1983).
41. C. Lin *et al.*, "Evidence of Network Demixing in GeS_2–Ga_2S_3 Chalcogenide Glasses: A Phase Transformation Study," *J. Solid State Chem.*, 184 [3] 584–588 (2011).